Buildup of III-V-compound semiconductor heterojunctions: Structural and electronic properties of monolayer-thick III-V overlayers on III-V substrates

J. M. Moison, C. Guille, M. Van Rompay, F. Barthe, F. Houzay, and M. Bensoussan
Laboratoire de Bagneux, Centre National d'Etudes des Télécommunications,
196 Avenue Henri Ravéra, F-92220 Bagneux, France
(Received 30 June 1988; revised manuscript received 18 October 1988)

We report an extensive study of the first stages of the buildup by molecular-beam epitaxy of III-V-compound semiconductor heterojunctions (AlAs, InAs, and GaAs with each other, and GaAs/GaP and InAs/InP). Surface-sensitive techniques have been applied *in situ*, first to yield information on the geometry and crystal structure of monolayer-thick overlayers of a III-V compound grown upon another III-V substrate. For atomically well-defined heterointerfaces, the buildup of the electron states at the interface has then been analyzed. In these cases, with respect to the vacuum level, the substrate band structure remains stationary, and the overlayer surface- and bulk-derived electron states appear at the position they have in the bulk overlayer material, within a ± 0.1 eV accuracy limit. The band offsets that we deduce are in good agreement with the electron-affinity rule and with recent experimental and theoretical data.

I. INTRODUCTION

In the last few years, the properties of heterojunctions between III-V compound semiconductors have been thoroughly studied. Progresses have been closely linked to improvements in growth techniques such as molecular-beam epitaxy (MBE), which can now build multilayer stacks or microstructures which are pure, ordered composition-controlled on an atomic scale, and tailored for fundamental studies or electronic devices. A great deal of attention has been particularly devoted to the determination by optical or transport measurements of the basic electronic parameter of the interface, the band lineup, or band offset, especially in the critical system $GaAs/Ga_{1-x}Al_xAs$.[1] On the other hand, rather little is known on the heterointerfaces at an atomic scale and on the way they are built. Oddly enough, in spite of a long tradition of tackling such problems with the tools of surface physics, *in situ* observations of electronic properties during the first steps of III-V heterostructure growth are scarce,[2] and are mostly limited to one system and /or one surface technique.

We present here what is to our knowledge the first effort to study the first steps of the buildup of most common III-V-compound semiconductor heterojunctions (AlAs, GaAs, and InAs with each other along [100]) by combining basic surface analysis techniques giving information on structural and electronic features, such as low-energy electron diffraction (LEED), Auger-electron spectroscopy (AES), x-ray and uv photoemission spectroscopies (XPS, UPS), and electron-energy-loss spectroscopy (EELS). We first check the structural properties of the interface such as interface flatness, interface abruptness, evolution of surface reconstruction, influence of strain, etc. For interfaces which may be considered as flat and abrupt, we then consider electronic properties such as buildup of overlayer electron states, behavior of substrate states, band lineup, or surface recombination. While particular results are in agreement with previously published data, the whole set of results gives new and simple indications about the general framework possibly encompassing the buildup of this whole class of heterostructures.

II. EXPERIMENTAL BUILDUP OF THE OVERLAYER-SUBSTRATE STRUCTURES

Sample structures will be referred to as overlayer-substrate structures. Since a III-V crystal in the [001] direction is made up of alternate atomic planes of third-column and fifth-column elements, our overlayer thickness unit, the monolayer (ML), is taken as the combination of two such substratelike planes. Structures are built in a Riber 2300 MBE chamber, under monitoring by 10-keV reflection high-energy electron diffraction (RHEED). The growth chamber is directly connected to an analysis ultrahigh-vacuum chamber equipped with a Vacuum Generators CLAM 100 electron-energy analyzer. The base crystals are (001) n-type (10^{18} cm^3) InP, GaAs, and GaP wafers. Overlayers of arsenides on phosphides are obtained through As/P exchanges by annealing under an As flux (equivalent pressure 10^{-5} Torr) chemically polished (InP) or ion-cleaned (GaP) substrates, at a temperature (550 °C) where surface P atoms desorb and are replaced by incoming As atoms.[3] Overlayers of arsenides on arsenides are obtained by classical MBE (Ref. 4) on thick buffer layers (>1000 Å) nonintentionally doped (residual doping level $p \leq 10^{15}$ cm^{-3}). The growth rate for arsenides is calibrated by RHEED oscillations during homoepitaxy from 0.05 ML to 1 ML/s and extrapolated to the desired values following an Arrhenius law with cell temperature. In some cases, this extrapolation has been slightly corrected in view of AES and XPS results. Growth conditions depend on the desired structure and follow some common classical rules. Thin (≈ 1 ML) overlayers are built at a growth rate of ≈ 0.05 ML/s, and

buffer layers at ≈ 1 ML/s. Growth temperatures lie around 600 °C, except for In-containing structures where it is reduced to 450 °C in order to avoid In desorption. Arsenic pressures are tuned during growth in order to obtain the "As-stabilized" regime except for In-containing layers where the maximum pressure ensuring an "In-stabilized" growth is used. The final thickness of the buffer layers is large enough to avoid effects of the initial contamination and to accommodate the eventual lattice mismatch, thus yielding unstrained substrates.

After cooling down, most often under As pressure down to 300 °C and then under vacuum down to room temperature (see Sec. III C), the structures are transferred to the analysis section and probed by LEED, AES, XPS, UPS, and EELS. All electronic spectra are obtained with the CLAM 100 analyzer. AES is performed with a primary electron energy of 2 keV and a modulation of 2.5 V and EELS with 120 eV and 1 V, respectively, XPS with the natural Al $K\alpha$ line of an x-ray source (1486.6 eV), and UPS with the 21.22 and 40.81 eV lines of a He lamp. The wavelength-integrated photoluminescence yield of GaAs and InP is also measured *in situ*, which gives the surface recombination velocity.[5] All results are referred to those obtained on pure binary samples, i.e., cleaned and annealed phosphide crystals and MBE-grown arsenide buffer layers. A few arsenide ternary alloys have also been grown for comparison purposes.

III. STRUCTURAL PROPERTIES OF OVERLAYER-SUBSTRATE SYSTEMS

A. Geometry

Since most structures except GaAs/AlAs and AlAs/GaAs involve a high lattice mismatch M between overlayer and substrate materials (referred to the overlayer parameter), we deal with strained growth. One of the first descriptions of this growth and a still valid one after some refinements[6] is the Franck–Van der Merwe and Matthews (FVM) description. In this model, as long as the overlayer thickness lies below a critical value, the overlayer is elastically distorted in order to assume the substrate parameter in the growth plane (pseudomorphism). Above this critical thickness, the strain is relaxed by generation of misfit dislocations. At another thickness often similar to the former, layer-after-layer growth is replaced by island growth, and deformations of the islands and of the substrate near the islands help relieve the strain. At high mismatches, both critical thicknesses lie in the ML range and the growth mode is known as the Stranski-Krastanov one. When they lie below 1 ML, island growth is obtained at once (Volmer-Weber growth mode). For our purpose, we must clearly avoid this last mode, so critical thicknesses must lie significantly above 1 ML. The critical mismatch where a ML becomes unstable has been calculated in the FVM approach, which was indeed originally limited to ML-thick overlayers, to be 10–15%.[7] The extrapolation of data obtained for smaller M (Ref. 8) also indicates a value larger than 10%. Therefore, since the mismatches involved in this work all lie below 7%, ML-thick overlayers should be stable. This point has been checked first by RHEED. Except for the initial stages of the buffer layer buildup, RHEED patterns always display short streaks, even at the overlayer completion, indicating planar layer-after-layer deposition (Fig. 1). The integer-order streak spacing corresponds to the expected lattice parameter of buffer layers, with an accuracy of $\pm 3\%$, which confirms the pseudomorphic deformation of the overlayer. Some samples (InAs/GaAs) have been observed by transmission electron microscopy (TEM) which revealed no particular feature down to the 50-Å scale. Finally, AES and XPS data which will be described further on confirm the overlayer flatness. It may be noted that the transition to the relaxed growth is abrupt and unambiguously observed (appearance of spots in RHEED, of islands in TEM, and of strong deviations from the planar model in AES and XPS). For the most mismatched system (InAs/GaAs), these various symptoms appear at ≈ 2 ML.[9] For the nearly matched systems GaAs/AlAs and AlAs/GaAs, they are not significantly detected whatever the thickness. It is then expected on both theoretical and experimental grounds that all structures are reasonably planar, even on an atomic scale.

B. Chemical composition

A further preliminary check must be made on the actual composition profile of the structures. For arsenides, evidence is now piling up of the occurrence of surface segregation phenomena at heterointerfaces.[10] We have analyzed this process in detail by AES and XPS for InAs/GaAs and GaAs/InAs interfaces[11] and shown that while the first one is abrupt, the second one is not. At the deposition of the first GaAs ML, a large fraction S ($\approx 80\%$) of the underlying In atomic layer segregates to the surface, thus burying the same fraction of the deposited Ga layer. The GaAs/InAs structure is then unstable with respect to chemical composition and the corresponding heterointerface is diffuse. Similar measurements for all arsenide heterointerfaces and ternary alloys, confirmed by UPS and EELS data, will be reported in detail elsewhere. They show for instance that $Ga_{1-x}Al_xAs$ surfaces are nearly pure GaAs while $Al_{1-x}In_xAs$ and $Ga_{1-x}In_xAs$ surfaces are nearly pure InAs. They also indicate that, except for GaAs/InAs and AlAs/InAs, all overlayer-substrate structures are chemically abrupt at the ML scale. This is in agreement with general segregation data[10] and with optical data on the thickness of quantum-well interfaces in $GaAs/Ga_{1-x}Al_xAs$ structures.[12]

In Table I, we present a part of these results, i.e., the $I(A^{III})/I(As)$ AES and XPS intensity ratios in our structures, reduced to their values in A^{III}-As substrates, together with theoretical expectations for $S=0$ and $S=1$. The simple model used here involves planar layers and an exponential absorption of emitted electrons scaled by the electron escape length. This unsophisticated model yields correct predictions for systems without segregation, which also confirms the thickness and the flatness of the overlayers. In the other cases, there is a strong indication of $S \approx 1$. Finally, for arsenides on phosphides, the over-

layer thickness is *a priori* unknown, and $I(A^{V})/I(B^{III})$ reduced ratios are compared with predictions for various values. Data for the InAs/InP case have been reported previously in detail[3] and are quite similar to those of the GaAs/GaP case: for all signals having probe depths between 5 and 20 Å, a fair agreement is obtained with a 2 ML thickness, indicating that these overlayers also are flat and pure arsenides, and that the As-P exchange is limited to the two topmost P layers. Finally, in all cases where surface segregation within arsenides is not operative, the structures appear to be as they have been planned to be, and their crystal structure and electronic properties can be discussed as for two-dimensional systems, at least to the first approximation.

C. Crystal structure

The surface reconstruction of all structures has been determined by RHEED, checked in some cases by

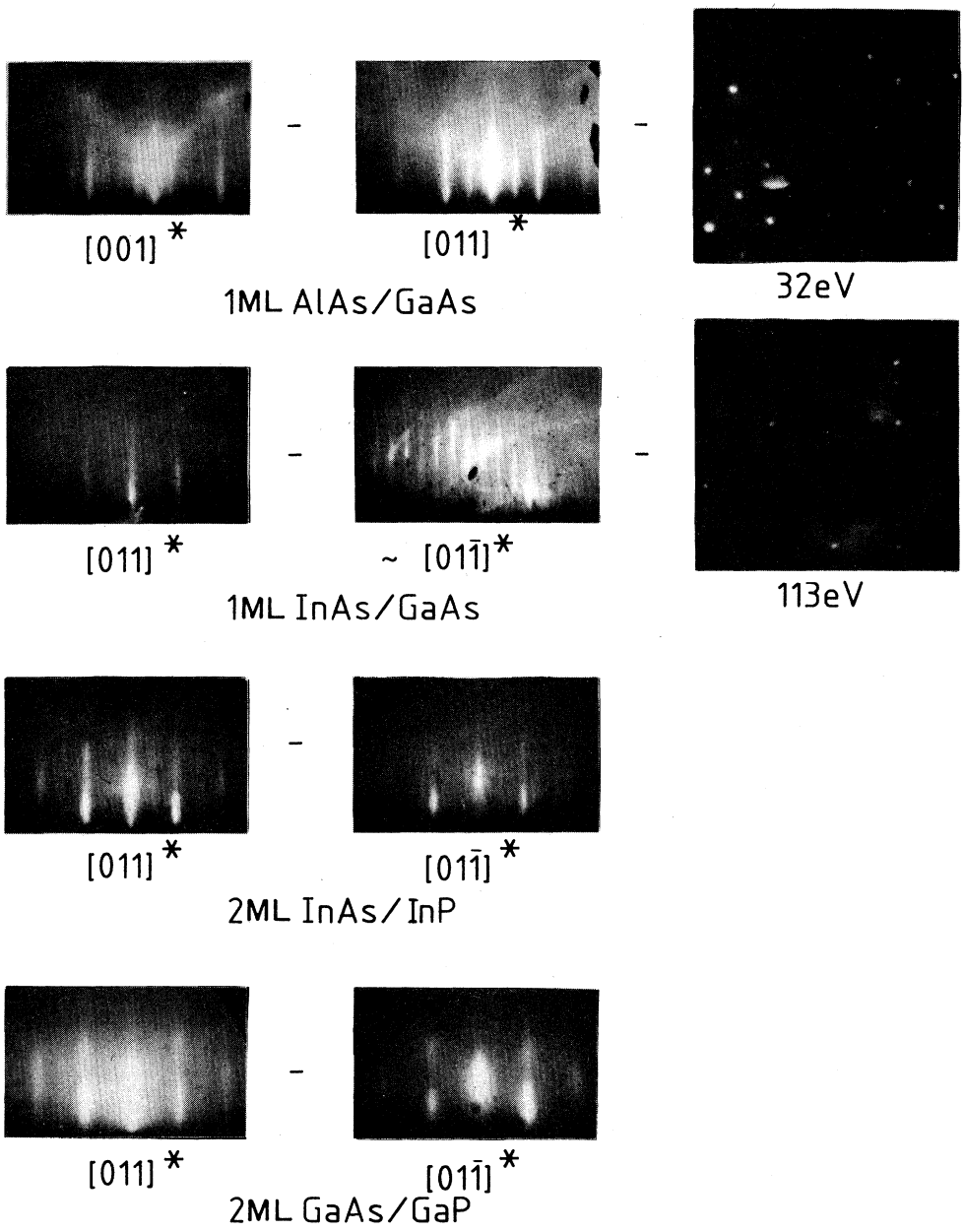

FIG. 1. Room-temperature electron-diffraction patterns of various overlayer-substrate structures: $c(4\times4)1$ ML AlAs/GaAs, $(2\times3)1$ ML InAs/GaAs, $(2\times4)2$ ML InAs/InP, and $(2\times4)2$ ML GaAs/GaP. The primary energy is 10 keV for RHEED patterns and is indicated under each picture for LEED patterns. Crystallographic directions indicated for RHEED patterns are normal to the picture plane.

LEED, and compared to the one of the substrate and overlayer materials. Some selected examples are shown in Fig. 1. Electron-diffraction patterns for arsenide structures at ML coverages are slightly less contrasted than those of the substrate buffer layers involved, while for arsenide-phosphide structures they are significantly degraded, although the surface unit mesh may be unambiguously obtained. As mentioned above, the integer-order streak spacing corresponds to the expected lattice parameter of buffer layers within $\pm 3\%$, which confirms the pseudomorphic deformation of the overlayer. Concerning the surface reconstruction, we deal here with arsenide surfaces for which the reconstruction is controlled by the As coverage. This coverage in turn depends on the substrate temperature T and As pressure P through a Langmuire combination $P\exp(E_d/kT)$ where E_d is the As desorption energy, as shown by the (T,P) phase transition curves[13,14] (see Fig. 2). The equilibrium reconstruction observed at low T and high P, which corresponds to the saturation As coverage, may in general be maintained at room temperature and under vacuum if adequate (T,P) paths for reducing T and P are followed. All measurements are performed on these surfaces. However, care must be exercised, for instance, in the case of GaAs or AlAs surfaces, since the (T,P) metastability region widely increases with decreasing temperature. The low-T, high-P overlayer reconstructions are listed in Table II together with the ones of the bare substrates; the various reconstructions obtained at higher T or lower P are also listed.

Under the assumption of total pseudomorphism of the overlayer with respect to the substrate, the deformation of the surface in its plane is given by the surface-bulk mismatch M. With respect to this parameter, the results of Table II may be summarized as follows. For low-M values ($M<3.5\%$), the surface unit mesh is not altered by the underlying substrate which stresses it. The MBE "phase diagram"—(T,P) lines of surface phase transition—is even unchanged: for instance, it is similar for GaAs or GaAs/AlAs ($M\approx 0\%$) or even InAs and InAs/InP ($M\approx 3\%$) (Fig. 2). At higher mismatches, the unit mesh is changed and the phase diagrams are displaced though their shape which is dictated by the desorption energy remains the same.[13,14] In two cases (InAs/AlAs and InAs/GaAs), reconstructions incommensurate with the bulk even appear. We have observed such transitions at $M\approx 4\%$ in InAs/$Ga_xIn_{1-x}As$ structures with $0\le x\le 1$.[14] The onset of such phase transitions at only 3–4 % while theoretical calculations yield much higher values confirms the presence of a built-in strain in surfaces of free materials as previously suggest-

TABLE I. Peak intensity ratios $I(A^{III})/I(As)$ in structures reduced to their values in the A^{III}-As substrates, with the corresponding electron escape depth (L). Experimental ratios are compared to expectation values for no surface segregation ($S=0$) and complete segregation of the top ML ($S=1$). Normal lattice parameters (Å) for the overlayer and substrate materials estimated in the elastic regime for total pseudomorphism are included. The best-fitting assumption is indicated by an arrow.

Peak	Ga AES	Ga XPS	In AES
L (Å)	5.0	7.5	9.6
1 ML InAs/GaAs (6.87 Å/5.65 Å)			
Experiment	0.53	0.73	0.34
→Model $S=0$	0.50	0.63	0.30
Model $S=1$	0.72	0.75	0.22
1 ML GaAs/InAs (4.85 Å/6.06 Å)			
Experiment	0.21	0.21	0.80
Model $S=0$	0.38	0.28	0.78
→Model $S=1$	0.21	0.18	0.84

Peak	Al AES	In AES
L (Å)	5.0	9.6
1 ML InAs/AlAs (6.87 Å/565 Å)		
Experiment	0.54	0.24
→Model $S=0$	0.50	0.30
Model $S=1$	0.72	0.22
1 ML AlAs/InAs (4.92 Å/6.06 Å)		
Experiment	0.26	0.95
Model $S=0$	0.38	0.75
→Model $S=1$	0.21	0.84

Peak	Ga AES	Al AES	Ga XPS
L (Å)	5.0	5.0	7.5
1 ML AlAs/GaAs (5.65 Å/5.65 Å)			
Experiment	0.59	0.60	0.57
→Model $S=0$	0.57	0.43	0.69
Model $S=1$	0.75	0.25	0.78
1 ML GaAs/AlAs (5.65 Å/5.65 Å)			
Experiment	0.40	0.61	0.33
→Model $S=0$	0.43	0.57	0.31
Model $S=1$	0.25	0.75	0.22

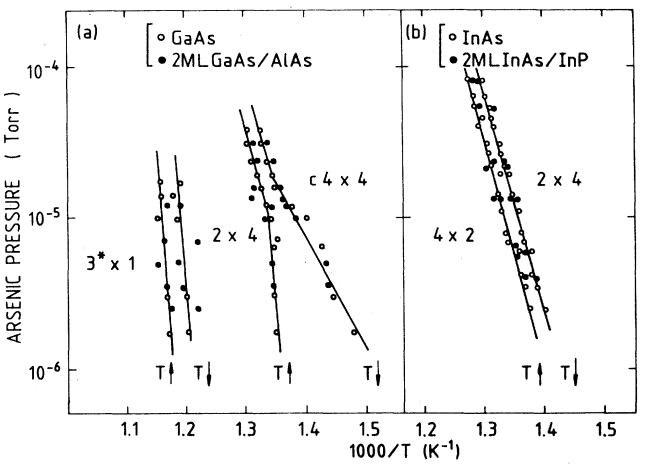

FIG. 2. (Temperature, arsenic pressure) Arrhenius diagram for the phase transitions of surfaces of (a) GaAs on its own bulk and on AlAs, and (b) InAs on its own bulk and on InP. At a given pressure, the temperature is scanned upwards or downwards, showing an hysteresis cycle; transition curves are noted accordingly. The $3^*\times 1$ GaAs superstructure corresponds to a commensurate 3×1 or incommensurate phase similar to the $2\times 3^*$ observed on InAs (Ref. 14).

TABLE II. Reconstructions of substrates and of overlayer-substrate structures, observed under various As pressure and temperature conditions: low temperature-high As pressure (LT-HP), and high temperature-low As pressure (HT-LP). 2×3* is a nearly 2×3 incommensurate structure (Ref. 14). The parameter mismatch M between substrate and overlayer unstrained materials are also indicated.

Overlayer / substrate	InAs / InAs	InAs / InP	InAs / GaAs	InAs / AlAs	GaAs / GaAs	GaAs / AlAs	GaAs / GaP	AlAs / AlAs	AlAs / GaAs
M (%)	0.0	−3.1	−6.7	−6.7	0.0	0.0	−3.6	0.0	0.0
LT-HP	2×4	2×4	2×3	2×3	c4×4	c4×4	2×3	c4×4	c4×4
HT-LT	4×2	4×2	2×3*	2×3*	2×4	2×4	?	3×2	3×2

ed.[15] Finally, it may be mentioned that the evolution of the reconstruction with overlayer thickness also depends on M. At low M ($M \approx 0\%$ for AlAs/GaAs and GaAs/AlAs), a correct epitaxy proceeds without change in reconstruction. At higher mismatches ($M \approx 7\%$ for InAs/GaAs and InAs/AlAs), the growth regime switches very rapidly to island growth and reconstructions are no longer significant; our experiments on InAs/$Ga_xIn_{1-x}As$ have nevertheless shown that for all x and hence for all M ($0\% \leq M \leq 7\%$) the reconstruction does not depend on the overlayer thickness up to the beginning of the island growth.[14] This confirms that this reconstruction is mostly controlled by the lattice parameter of the bulk—i.e., by M—and not by its chemical nature which varies between the first ML and the next ones.

IV. ELECTRONIC PROPERTIES

A. UPS data and occupied states

The electronic properties of the structures at room temperature and under vacuum have been deduced from the UPS and EELS spectra. Since all observations made on the arsenide-phosphide structures indicate that the control on their quality is lesser than for arsenide-arsenide structures, and also in view of their lesser present interest, our effort has been concentrated on the latter. We first report the results on occupied states obtained by UPS. The valence-band density of states (DOS) is deduced from the 21.22-eV (He I) spectrum after removal of an exponential contribution of secondary elec-

TABLE III. DOS characteristic energies (eV) below the vacuum level for III-V substrates. CB-I, CB-II, VB-I, and VB-II are conduction- and valence-band features, CL are the In and Ga core levels and CL* their mean weighted energy, E_V and E_C are the band-gap edges, E_F is the Fermi level, VBF-I′ and VBF-I″ are determinations of the valence-band feature VBF, ESS′, and ESS″ are determinations of the empty surface band ESS, and OSS is the top of the highest occupied surface band. The surface or bulk (s or b) origin of the features and their determination procedure are indicated at the left-hand side; a–g letters refer to corresponding EELS peak energies (see Fig. 8).

	b	E_g	AlAs 2.17	GaAs 1.42	InAs 0.36	GaP 2.26	InP 1.35
CL*−g−E	b	CB-II		0.05	−0.08	0.05	−0.08
CL*−f−E	b	CB-I		2.25	2.12	2.05	2.42
CL−e−E	s	ESS′		3.55	3.58	3.75	3.18
VB-II-d	s	ESS″	4.05	3.55	3.70	3.45	3.60
UPS	b	E_C	3.78	4.18	5.14	3.54	4.40
UPS	s	E_F	4.95	4.90	4.85	4.85	4.75
UPS	b	E_V	5.95	5.60	5.50	5.80	5.75
UPS	s	OSS				5.50	5.50
CB-I+b	b	VBF-I′		5.95	5.42	6.25	6.02
CB-II+c	b	VBF-I″		6.15	5.62	6.05	5.62
ESS+a	?	VBF-II	7.15	6.75	6.44	6.40	5.89
UPS	b	VB-I	7.12	6.70	6.75	7.47	7.25
UPS	b	VB-II	11.65	12.25	11.50	12.45	11.40
UPS	b	CL In $4d_{5/2}$			22.35		22.35
UPS	b	CL* In			22.67		22.67
UPS	b	CL In $4d_{3/2}$			23.20		23.20
UPS	b	CL Ga $3d_{5/2}$		24.20		24.20	
UPS	b	CL* Ga		24.35		24.35	
UPS	b	Cl Ga $3d_{3/2}$		24.60		24.60	

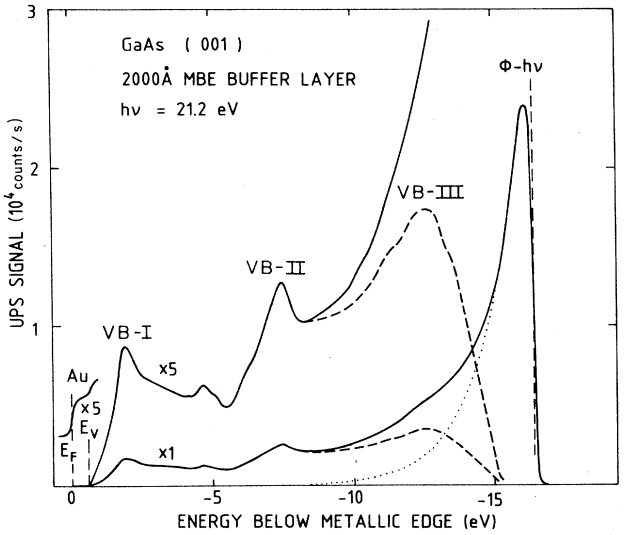

FIG. 3. Example of a typical UPS spectrum (solid curve) and of the corresponding UPS-derived valence-band DOS (dashed curve) obtained after removal of an exponential contribution of the secondary electrons of the form $\exp(E-E_F/kT)$ (dotted curve). The origin of the energy scale is the Fermi edge of a metallic sample drawn in the left-hand side.

trons[16] fitted on the low-kinetic-energy side of the spectrum (see an example in Fig. 3). This fit is not critical and merely helps enhancing low-kinetic-energy features. The In 4*d* and Ga 3*d* core levels are obtained from the 40.81-eV (He II) spectrum (see an example in Fig. 4). Though rather reproducible, the shape of the spectra will not be discussed quantitatively here. The noise on a single spectrum may be seen in Fig. 6.

All UPS-derived DOS obtained are similar, and the spectra obtained on pure binary compounds are in fair agreement with previous determinations. The valence-band DOS displays three main peaks (VB-I, VB-II, and

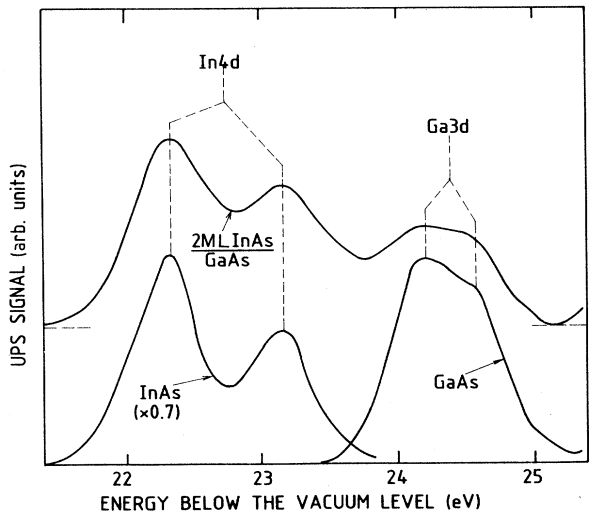

FIG. 4. UPS-derived Ga 3*d* and In 4*d* core levels referred to the vacuum level for InAs, GaAs, and 2 ML InAs/GaAs.

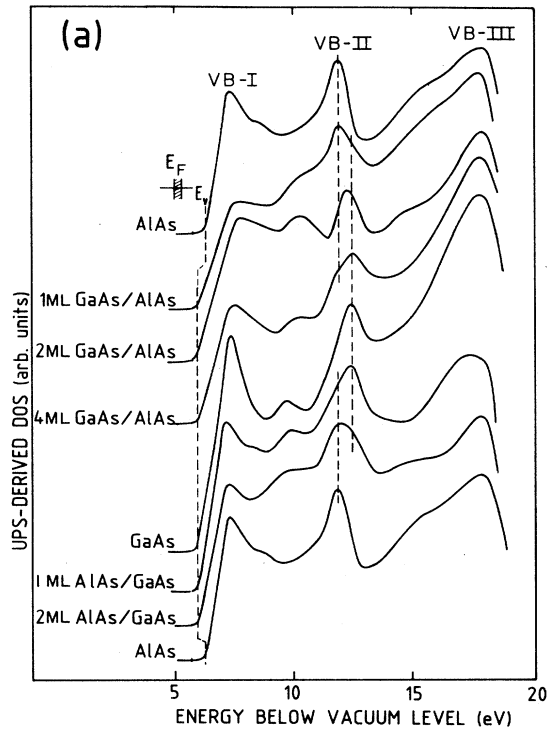

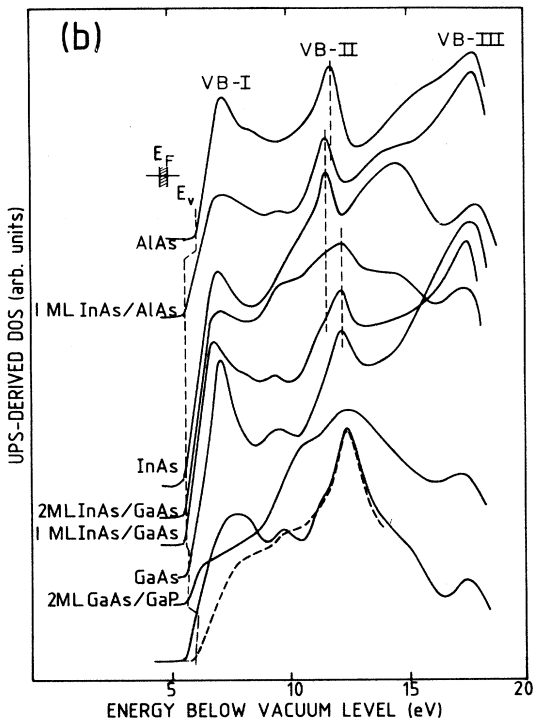

FIG. 5. UPS-derived valence-band DOS for substrates and overlayer-substrate structures: (a) GaAs/AlAs and AlAs/GaAs, (b) InAs/GaAs, InAs/AlAs, InAs/InP, and GaAs/GaP. The dashed spectrum corresponds to GaP exposed to 10^4 L [where L = Langmuir (1 L = 10^{-6} Torr sec)] of oxygen, which removes the near-VBM surface contribution and yields the true position of the GaP VBM.

VB-III) as expected for the bulk of III-V compounds from theoretical calculations.[17] The oxygen-adsorption test has been used on the pure binary compounds in order to separate the contribution of surface states and bulk valence-band states in the UPS-derived DOS (see for instance the GaP case in Fig. 5). The surface state contribution is found to be particularly important near the top of the valence band: peak VB-I is mostly bulk derived in AlAs and InAs,[18] mostly surface derived in GaP and GaAs, and composite in InP (see Fig. 5 and Ref. 18). In these last two cases, its position depends on the final surface treatment. On the other hand, VB-II has a definite position and an unambiguous bulk origin in binary compounds. VB-III seems to have the same properties but its position is a little too dependent on the background subtraction fit to be of accurate use. Other peaks are either associated to surface states or not obtained reliably enough. Finally, the position E_V of the valence-band maximum (VBM) is obtained by linear extrapolation to zero of the DOS, taking care that no important surface-derived DOS is present in the extrapolation range. In principle, the UPS-derived DOS should be fitted with a power law of $(E-E_V)$ but the exponent cannot yet be unambiguously chosen[19] though it may certainly differ from unity. However, the shape of the UPS-derived DOS is actually fairly linear in an ≈ 1 eV range in all cases, and the use of the same procedure for determining E_V should yield with a correct accuracy the relative positions of the various VBM's. Furthermore, the ionization energies we obtain are in good agreement with determinations by other methods.[20]

Our main concern here will be the overlayer-induced DOS and its energy relation to the substrate DOS. The energy scaling for UPS spectra must be accurate, realistic, and common to all the substrates and to all the structures. This is a rather complicated problem to which no clear-cut answer has been given up to now. Three "energy references" are commonly used,[1] the Fermi level, the core levels, and the vacuum level, each of them having advantages and drawbacks. The Fermi level E_F is the most straightforward choice. Since all samples are fair conductors connected to the electrical ground of the experimental setup, their Fermi levels are aligned on the spectrometer energy scale. This position may be obtained with a good accuracy—and is regularly checked—from the Fermi edge of the UPS spectrum of a clean gold sample (see Fig. 3). If E_F is to be used as the only reference for band lineup purposes, it requires in principle (E_F-E_V) to be stable for a given material whatever the changes of surface conditions (for the substrate material) or of thickness and underlying substrate (for the overlayer material). There seem to be no reason for which this condition should be fulfilled for the overlayer. For the substrate, the Fermi level at the surface—as probed by UPS—is most usually pinned somewhere inside the band gap by the gap surface states; its position with respect to the bulk band structure then depends in principle on the changes of the surface states as the overlayer grows, which may lead to a modified pinning or even to unpinning. Such displacements which are commonly observed[21] require the use of valence-band features for band lineup determination, which complicates the comparison between many systems.

Another possible energy reference, seemingly universal, is the vacuum level E_{vac}, understood in photoemission experiments as the potential experienced by the free photoelectron just outside the solid. This level may be set in the previous E_F related energy scale through the work function Φ $(=E_{\text{vac}}-E_F)$, which is determined from the distance in the UPS spectra between the "Fermi level" and the low-kinetic-energy cutoff $(=E_{\text{photon}}-\Phi)$. In our spectra, the width of the cutoff, which is related to the homogeneity of Φ, is ≈ 0.15 eV for arsenide structures and ≈ 0.4 eV for phosphide-based structures, to be compared to the resolution-limited width of the metallic Fermi cutoff ≈ 0.15 eV. This second energy reference is then less accurate than the first one, but is presumably less sensitive to uncontrollable displacements due to Fermi-level pinning or unpinning. Its application to our case requires the ionization potential of a material E_i—and no longer $E_F-E_V=E_i-\Phi$—to be stable under the changes undergone by the materials. For the overlayer material, there is again no *a priori* reason for this behavior. For the substrate material, the condition is often checked, though this is certainly not the rule; consider for instance the extreme case of surfaces activated to "negative electron affinity" by alkali adsorption.

The third common energy reference is given by atomic-like core levels (CL), whose position may be obtained throughout the structure growth procedure and with a good accuracy from the UPS spectrum. Their relation to the valence band $(E_V-\text{CL})$ is in principle a constant of the material as soon as it has acquired its bulklike band structure, which gives an excellent procedure for the determination of band lineups. However, in practice, core levels may be distorted—sometimes drastically—by chemical shifts due to different bonding configurations in the bulk and at the surface or at the heterointerface, thus requiring a difficult line-shape analysis. However, since all our surfaces are As-saturated at room temperature, we do not expect the surface shifts on the core levels of the

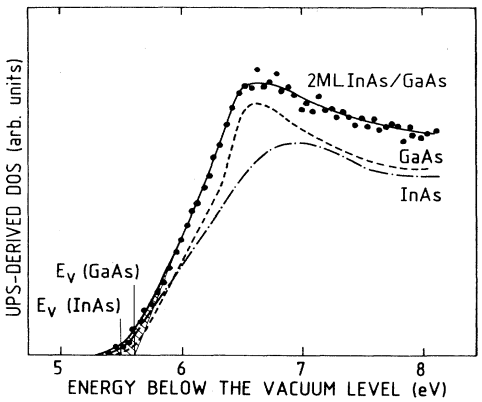

FIG. 6. Enlargement near the VBM of UPS-derived valence-band DOS for GaAs, InAs, and 2 ML InAs/GaAs. The hatched area is the near-VBM contribution of the InAs overlayer.

third-column atoms—which are buried—to be important. For instance, the Ga $3d$ core level surface shift is reported to be very small (<0.05 eV) on MBE-grown (100) GaAs, as indeed on cleaved, i.e., mixed surfaces, with respect to those reported for the As core level (≈ 0.5 eV).[22] The surface contribution therefore does not change the core level position nor line shape. The slight evolution of the line shape (widening) of Ga or In core levels that we observe on some structures may then be attributed to an heterogeneity of $(E_F - \mathrm{CL})$ in the surface plane. This is confirmed by the excellent stability (± 0.05 eV) of the separation of In and Ga core levels throughout the variety of structures under study (see an example in Fig. 4).

Since none of the three procedures seem *a priori* completely foolproof, we tried all of them in our data evaluation, with reproducibility as our first criterion. For substrates, surprisingly enough, we did not find any significant difference between the three procedures, within a ± 0.1 eV accuracy range. For structures, the situation is more complex. The difference between core levels and the vacuum level is very stable (± 0.05 eV) except in a few cases where a clearly incorrect value of Φ shifts the whole band structure with respect to the "wrong" vacuum level. The Fermi level fluctuates rather strongly—up to ± 0.15 eV for a given structure—with respect to the other possible references and on the whole seems to be a slightly worse reference. The core levels seem then to be the first choice, as already concluded in the previous section. However, we cannot obtain any Al core level with our uv source, so that we have finally chosen a mixed solution. In and/or Ga core levels are taken as the energy reference, except for the AlAs substrate where core levels are not available and for which we use the next-lowest sharp structure VB-II. In all cases, this procedure minimizes the dispersion on the position of band-structure features such as E_V, VB-II, and VB-III, to about ± 0.07 eV for a given substrate or structure.

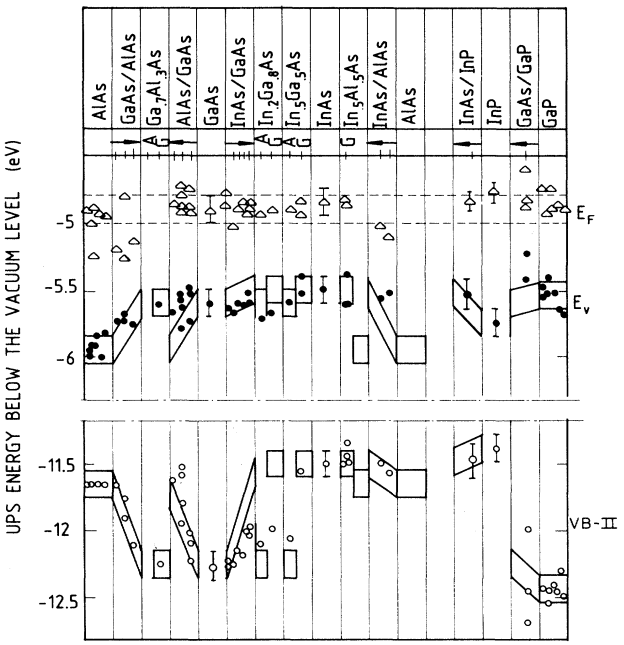

FIG. 7. Energy position with respect to the vacuum level of the Fermi level E_F (triangles), of the valence-band edge E_V (open circles), and of the valence-band peak VB-II (open circles), deduced from UPS spectra for various overlayer-substrate structures and substrates. For structures, the arrows indicate increasing overlayer thicknesses: 1, 2, and 4 ML for GaAs/AlAs, 1, 1.5, and 2 ML for AlAs/GaAs, 1, 1.5, 2, 7, and 3 ML on a InAs/GaAs short-period superlattice grown on InP for InAs/GaAs, and 2 ML for GaAs/GaP and InAs/InP. For ternary alloys, G and A letters indicate, respectively, as-grown samples and samples annealed above the temperature of desorption of the less bonded atom (In for $Ga_{1-x}In_xAs$ and $Al_{1-x}In_xAs$, Ga for $Ga_{1-x}Al_xAs$). Symbols with error bars represent the combinations of many experimental data for InAs, GaAs, and InP substrates. Boxes drawn around the symbols represent roughly the expected behavior, i.e., for structures evolution from substrate to overlayer position, and for ternary alloys the position corresponding to the segregating species in as-grown (G) samples and to the nondesorbing species in annealed (A) samples.

The zero of the common energy scale, on which In $4d$, Ga $3d$, and VB-II (AlAs) are rigidly related to each other and to the data, may still be chosen at will and is of no real importance. In order not to privilege a single system, and taking advantage of the good stability of the vacuum level in this energy scale throughout the samples, we choose its average position as the origin of the energy scale. In this scale, we have In $4d_{5/2} = -22.35$ eV, Ga $3d_{5/2} = -24.20$ eV and VB-II (AlAs) $= -11.65$ eV. Typically DOS features for each structure and for the materials which form its substrate and overlayer are shown in Figs. 5–7 with this common energy scale. It may be emphasized that this procedure is intended to yield more accurate results on a common energy scale for all samples, and that other choices lead to the same trends as those which will be presented in the next section. For instance, it may be seen in Fig. 7 that in the energy scale based on core levels or E_{vac}, E_F is approximately stable (± 0.1 eV); this shows that the same picture drawn with an energy scale based on E_F would display similar trends. This rather surprising though convenient agreement will be discussed in Sec. V.

B. Buildup of the overlayer valence band and band offset

We first discuss the evolution of the bulk-derived features VB-II and E_V during the buildup of structures, from the bare substrate and on. Obviously, the most straightforward interpretation can be made in the case of GaAs/AlAs and AlAs/GaAs structures which are potentially the smoothest ones due to the very low lattice mismatch involved and for which thick planar overlayers can be built. Indeed, the coarse position of VB-II clearly moves from its AlAs position to its GaAs position during the deposition of GaAs on AlAs [Fig. 5(a)] and conversely for the AlAs/GaAs structure. Furthermore, at intermediate thicknesses, GaAs-derived and AlAs-derived peaks can be still observed at their position in bulk GaAs and AlAs in the vacuum level energy scale and only their

relative weight changes, making their mean position evolute continuously. Like the stability of core levels, this shows that the bulk band structure of the substrate is not shifted significantly in energy during overlayer deposition. The case of InAs/AlAs and InAs/GaAs is complicated by the limitation of the overlayer thickness to ≈ 2 ML. The evolution of VB-II is small and clear only at thicknesses where islands appear. Finally, the high-kinetic-energy cutoff (apparent VBM) in UPS-derived DOS follows in all systems an evolution similar to the one of VB-II, from the VBM of the substrate towards the VBM of the thick overlayer material. Again, this evolution is clearer for GaAs/AlAs and AlAs/GaAs cases [Fig. 5(a)]: the GaAs VBM appears very early during the deposition of GaAs on AlAs while the appearance of the AlAs VBM during the deposition of AlAs on GaAs is delayed because of its mixing with states of the underlying GaAs. The apparition of an InAs-derived DOS above the VBM of GaAs for InAs/GaAs structures is fairly visible too (see Fig. 6). Such spectra have been used for a long time in order to determine heterojunction band offsets[21] and we discuss them now in this respect.

Considering the depth probed by UPS (≈ 3 ML), our results show that, even if the overlayer bulk band structure is fully established only at thicknesses of ≈ 4 ML, the overlayer-derived states which appear below this thickness are already at their final position in the thick layer. In other words, the heterointerface is already "formed" at the first stages of its buildup, like it is observed for metal-semiconductor contacts. This is reasonable, considering the common nature of all materials involved, and it indicates that surface dipoles are similar and cancel to a zero interface dipole. It also considerably simplifies the interpretation of results in terms of band offset, since it means that the actual band offset obtained for the completed heterojunction should be fairly well approximated by the difference of the ionization energies (electron-affinity rule[1]). From our data, we can deduce "band offset" values from (1) the electron-affinity rule, (2) from the band structure of ternary alloys (see data in Fig. 7) following the method of Ref. 23, i.e., from a nonformed heterointerface, and (3) from the measurements performed on structures which involve a half-formed interface and a "DOS offset" rather than an actual band offset. All these determinations are in agreement with each other and yield 0.35 ± 0.07 eV for GaAs/AlAs and AlAs/GaAs, 0.1 ± 0.07 eV for InAs/GaAs, and 0.45 ± 0.07 eV for InAs/AlAs. Other experimental determinations of the band offset in fully formed heterojunctions by similar methods (XPS) are 0.35–0.45 eV for GaAs/AlAs, and 0.17 eV for InAs/GaAs,[2] in good agreement with our data.

C. EELS data and empty states

EELS spectra of III-V compound semiconductors have been often reported.[24] Spectra of structures are very similar to those of the substrates; their main characteristic peaks labeled a–g and p are shown in Fig. 8 and may be mostly interpreted in the same manner. For bare substrates, we have separated bulk- and surface-derived transitions by changing the primary energy and performing oxygen adsorption experiments. High energy-loss features f and g (≈ 20–25 eV) correspond to transitions from the topmost core levels (In $4d$ and Ga $3d$) to conduction-band features CB-I and CB-II involving a large exciton binding energy E. b and c peaks (≈ 4–7 eV)

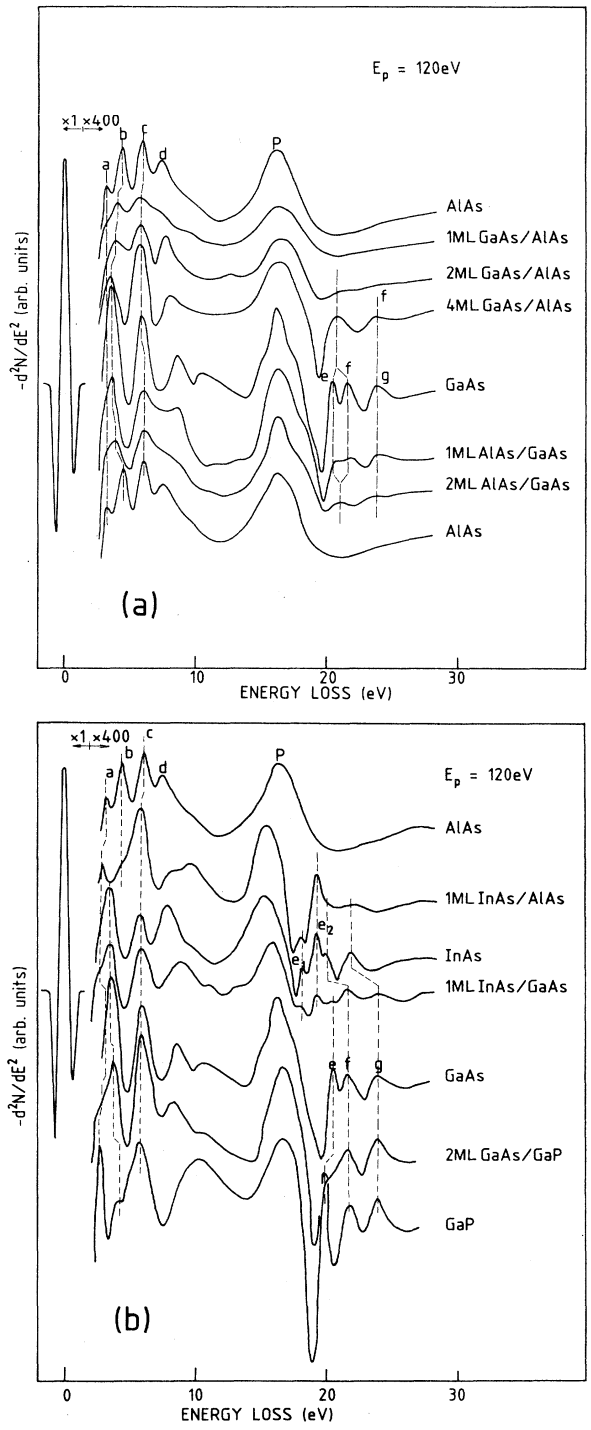

FIG. 8. EELS spectra obtained at a primary energy of 120 eV and a 1-eV modulation for (a) GaAs/AlAs and AlAs/GaAs, (b) InAs/GaAs, InAs/AlAs, InAs/InP, and GaAs/GaP structures. Peaks are labeled a–g and p for the bulk plasmon.

may be attributed to transitions between a valence-band feature VBF-I and CB-I or CB-II, and the large feature p ($\approx$15–17 eV) to the bulk plasmon. Other peaks are associated with the presence of the surface. The transitions towards a surface empty state band ESS associated with third-column surface atoms from VB-II and the core levels give rise to peak d ($\approx$8–9 eV), and to a doublet $[e_1,e_2]$ ($\approx$18–20 eV) involving also E which reduces to a singlet e for Ga-derived peaks for which the core level separation is lower. Peak a ($\approx$3 eV), which often appears as a shoulder in the neighboring bulk-derived peak b, corresponds to a transition promoting electrons to ESS from a valence-band feature VBF-II, which seems associated with VB-I for arsenides and VBF-I for phosphides (see Fig. 10). Finally, other peaks lying between 7 and 14 eV have been associated with the back bonds of surface atoms.[24] Positions of peaks a, b, c, p, e, f, and g for all structures and bulk materials are reported in Fig. 9 and indirectly in Table III. The accuracy with which they may be determined is $\approx$0.2 eV except for the wide plasmon peak for which it is $\approx$0.3 eV taking into account the primary energy drift during the measurements and the sample-to-sample reproducibility.

Since we know from UPS the absolute position of the occupied initial levels, the EELS transition energies give us the position of the empty final levels, taking E into account. Unfortunately, E is not accurately known. For the highest ($\approx$20 eV) transitions, we take the values of Van Laar *et al.*,[24] i.e., 0.5 eV for Ga-related transitions and 0.45 eV for In-related ones, although higher values have been proposed.[25] For lower-energy transitions, we assume that E is small ($<$0.1 eV). Our choice is supported by the fact that the two determinations of ESS (ESS′, ESS″) obtained from the two transitions e and d which involve it as a final level are in close agreement. Finally, all characteristic energies in empty or occupied DOS for substrates and structures are listed in Table III and shown in Fig. 10.

The trends in EELS peaks during heterojunction buildup must be considered in view of the penetration depth of the primary beam and the escape depth of backscattered electrons ($\approx$3 ML). The shifts of b, c, and p bulk-derived peaks may be understood simply as the progressive replacement of the peaks of the substrate by those of the overlayer material (Fig. 9). The most interesting information is obtained from e, f, and g peaks whose initial state (d core levels) are known from UPS to be stationary during structure growth. Figure 9 shows that peaks corresponding to the substrate or overlayer materials are found on structures approximately at their position on bare substrates. For instance, in the InAs/AlAs (respectively, GaAs/AlAs) structure, we observe the $\approx$22.3-eV (respectively, 21.6–23.8 eV) peak associated to the InAs (respectively, GaAs) conduction band. A similar situation is found on 1 ML InAs/AlAs and to a lesser extent on 1 ML GaAs/AlAs for which no Al-derived peak is

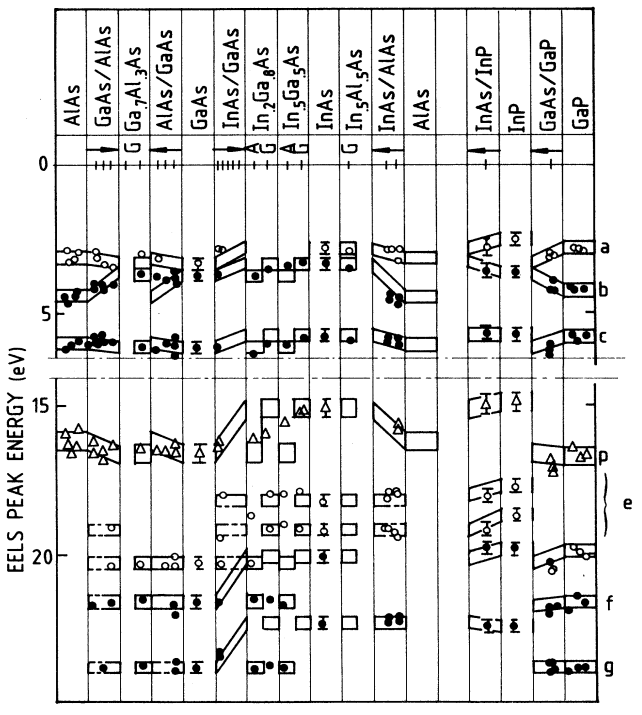

FIG. 9. EELS peak positions for various overlayer-substrate structures and substrates. a–g letters in the right-hand margin refer to peak identification in Fig. 8. Open circles indicate surface-derived transitions, solid ones bulk-derived transitions, and triangles the bulk plasmon. Sample identification is the same as in Fig. 7, and boxes are drawn around the symbols in the same manner.

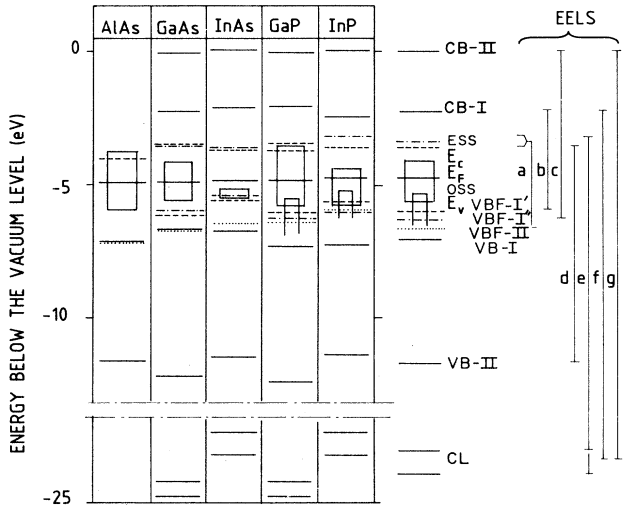

FIG. 10. Characteristic features of the band structure of AlAs, GaAs, InAs, GaP, and InP deduced from our UPS and EELS measurements, taken from Table III. The positions of d core levels (CL), of valence-band features (VB-I and VB-II), of the valence- and conduction-band extrema (E_V,E_C), of the Fermi level (E_F), and of an occupied surface state band (OSS) are obtained from UPS data. EELS peaks assigned in the right-hand margin give the positions of conduction band features (CB-I, CB-II), of an empty surface state band (ESS), and of bulk- or surface-derived valence-band features (VBF-I′, VBF-I″, and VBF-II).

present. This indicates that the empty states corresponding to the overlayer are already at their position in its bulk material where they form the conduction band, supposing that the exciton binding energy does not depend much on the material. Here again, we find that the basic electronic properties of the overlayer are formed at the very first stages of its buildup.

D. Surface states and Fermi-level pinning

As mentioned earlier, surface state contributions appear in the UPS and EELS spectra of bare materials. The spectra of structures also show indications of similar contributions, but sorting them from the contribution of the overlayer—which may be indeed considered as the surface in view of its thinness—is not at all straightforward, and may be actually illusory. However, a few indications exist, first in the UPS spectra. A large surface DOS which is located near the InP VBM and widely extends in its band gap disappears in the InAs/InP structure; in view of what we said about the replacement of substrate bulk states by overlayer ones, this may be associated with the absence of surface contribution in the InAs band gap (see Ref. 3 for details). For GaP where similar gap surface states appear, the high-kinetic-energy cutoff is nearly stationary during GaAs/GaP formation. This may be attributed to the simultaneous disappearance of the GaP-derived surface states which extend ≈ 0.3 eV in the band gap of GaP and to the buildup of the VBM of GaAs which no gap surface states are seen by UPS. Surface state replacement is observed only in these two systems where the substrate has visible gap surface states while the overlayer material has none. For the other structures, surface states located near the valence-band maximum and bulk DOS overlap and cannot be easily separated from each other. The only possible exceptions could be the GaAs and AlAs sharp surface state bands located at ≈ 1.1 eV below the respective VBM's; however, they overlap in GaAs/AlAs and AlAs/GaAs structures and are considerably widened and barely visible in GaAs/GaP so that those data again are not conclusive.

In EELS spectra, the only clear indication is given by the *e* peaks for which the initial states are the core levels and the final states a surface state band. Their stability in all samples indicates that, again if the exciton energy is not significantly changed by the underlying substrate, the surface state band of a given overlayer (InAs/GaAs, GaAs/AlAs, and InAs/AlAs) appears at the same position as in the thick overlayer material. Similar though less clear information may be extracted from the *d* peak for which final states lie in the same empty surface band and initial states in VB-II. We have already reported the same phenomenon for InAs/InP.[3] For AlAs/GaAs or GaAs/GaP, no such data is available, because of the lack of a core level in He II UPS spectra and/or to peak overlap so that data are not conclusive. Finally, the few data we have on the surface states of structures point to the same trend as for bulk-derived states, i.e., indicate that they are located approximately at the same energy as on the thick overlayer material. A similar trend is observed on the surface recombination velocity obtained from *in situ* photoluminescence. We have already shown that fitting an InAs overlayer on InP moves surfaces states out of the InP band gap and hence reduces the surface recombination velocity.[5] We report here that fitting this same overlayer of GaAs creates states inside the GaAs band gap and simultaneously increases this velocity.

Another indirect indication on surface states is provided by the position of the Fermi level E_F. No systematic study of the variation of its position with the bulk doping of structures has been performed; arsenide layers are nonintentionally doped ($p < \approx 10^{15}$ cm^{-3}), while InP and GaP substrates are heavily *n*-type doped ($n \approx 10^{18}$ cm^{-3}). However, the Fermi level was checked to be strongly pinned on InP and GaAs substrates by changing the bulk from heavy *n* doping to *p* doping and it is likely to be also pinned in structures by the overlayer surface states, if not by the probably much less numerous overlayer-substrate interface states. Indeed, it is found at approximately the same location in structures and in the overlayer materials. A more surprising piece of information is the near-perfect stability of the work function and hence of E_F throughout the samples: for most substrates, ternary alloys and structures, it lies at 4.9 ± 0.1 eV.

V. DISCUSSION

Our UPS and EELS data indicate a clear trend for the buildup of atomically well-defined III-V-compound semiconductor heterojunctions: with respect to the vacuum level, the band structure of the substrate remains stable, and the surface or bulk overlayer-derived electron states appear at the energies they have in thick unstrained overlayers. It must obviously be kept in mind that we have only a very restricted and perhaps distorted view of those states. The accuracy of UPS and EELS is limited to ≈ 0.1 eV. Furthermore, these techniques are sensitive only to large densities of states and not really to the smaller details of band structure. In this respect, they cannot really compete with transport or optical experiments for the accurate determination of these details. For instance, overlayer strain leads to splitting of heavy- and light-hole bands as shown by luminescence data.[26] We have tried to observe such effects by building an InAs/GaAs structure on a $Ga_{0.5}In_{0.5}As$/InP base, which redistributes the strain between GaAs (from 0 to $\approx 3\%$ extension) and InAs (from ≈ 7 to $\approx 3\%$ compression), but we found no significant influence of this redistribution on the "band offset" (see Fig. 7). This could be expected since the center of gravity of band maxima—and hence the UPS spectrum—has been shown to be nearly insensitive to strain.[27]

With this limitation in mind, in order to evaluate the accuracy of our results, it is worth comparing them to previous experimental data and general theoretical predictions involving all III-V systems in the issue of band lineup,[28,29] since this parameter is both widely studied and very sensitive. We have already mentioned in Sec. IV B that published photoemission data are in correct agreement with ours. However, we have not observed the influence of the growth sequence previously reported in GaAs/AlAs versus AlAs/GaAs systems.[2] Optical and

transport measurements yield 0.4–0.5 eV for the GaAs/AlAs band offset and 0.0–0.1 eV for the GaAs/InAs one,[1] in agreement with ours within the 0.1 eV accuracy limit. First-principles or tight-binding calculations of the GaAs/AlAs band offset[30] give results in the 0.35–0.50 eV range. Considering now general heterojunction models, we compare in Fig. 11 the VBM positions we obtain with those calculated by Tersoff[1,31] by alignment of the band structure "neutrality level," by Langer and Heinrich[32] by alignment of deep-impurity levels, by Cardona and Christensen[33] by alignment of a dielectric midgap energy, by Margaritondo *et al.*[29,34] by reference to actual heterojunctions with Ge, and other groups[35,36] (Si and Ge ionization energies are taken from Ref. 37). The overall agreement lies within the ±0.1 eV range which has been claimed by Margaritondo[29] to be the ultimate limit of such correlations.

On this basis, we feel that our conclusion on the buildup of electron states in the heterojunction is correct within this ±0.1 eV accuracy limit. Its first consequence is the applicability to band lineup of the old electron-affinity rule, which should actually be called here the "ionization energy rule," all the more since the actual value of the band gap of strained overlayers is not a trivial question. The revival of this rule has already been suggested by Margaritondo[29] considering the recent and simultaneous determinations of the ionization energies and of the band offset, more reliable than those opposing this rule. It may be reminded that we deal here with heterojunctions between III-V compounds which are very similar materials, with identical crystal structures and

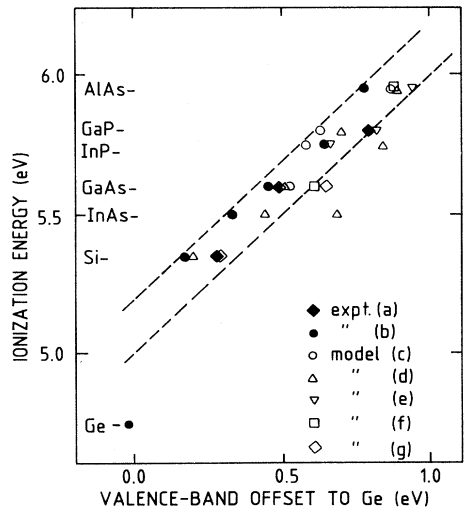

FIG. 11. Ionization energies deduced from our UPS data for III-V compounds or those of Sébenne *et al.* (Ref. 37) for Si and Ge band-offset values with Ge of the literature. Those values are obtained (a) from a review of experimental results (Ref. 34), (b) from UPS and XPS data (Refs. 22 and 28), (c) from calculations by Tersoff (Ref. 31), (d) by Cardona and Christensen (Ref. 33), and (e) by Langer and Heinrich (Ref. 32) (data aligned on the mean GaAs value 0.49 eV), (f) from tight-binding calculations by Haussy *et al.* (Ref. 35), and (g) by Harrison and Tersoff (Ref. 36). The slope-one lines are drawn to fit best the data within the ±0.1 eV accuracy limit, excluding the Ge point.

neighboring electronic structures, and that the interface is built with in principle neither broken nor wrong bonds. All this suggests that the surface dipoles should be similar and that interfact dipoles should be very small, as also shown by theoretical calculations.[30] These properties, which may be the privilege of III-V systems, make them ideal cases for UPS and EELS tests of the electron-affinity rule, but also of general models such as those mentioned above which ignore the possibility of interface dipoles or strain effects. They may also be the origin of the agreement between the predictions of all these models (Fig. 11). It may be noted here that a plot of ionization energy versus band gap for the five semiconductors considered here leads us to a ratio of the valence-band offset to the band-gap difference of 20±5 %, with the ±0.1 eV accuracy on E_V values. This ratio, though near the accepted value of 30% for GaAs/$Al_{1-x}Ga_xAs$,[1] is quite different from the 75% value observed for $A^{IV}/B^{III}C^{V}$ or $A^{IV}/B^{II}C^{VI}$ heterojunctions,[38] showing that care must be excercized in extrapolating results from one class of materials to another one.

It may also be argued, as suggested by the approach of Mailhiot and Duke,[39] that the validity of the electron-affinity rule, the validity of models involving the alignment of band-structure characteristic levels in heterojunctions or metal-semiconductor contacts, and even the stability of our experimental Fermi level, are manifestations of the same underlying physical phenomenon. All general theories of band lineup mentioned above involve the presumed existence in all materials of reference levels which merely need to be aligned to put all band structures on a common energy scale, which is conserved in the formed heterojunction if the interface dipole is negligible. The levels considered are the vacuum level, the core levels,[23] the neutrality level[31] (≈center of gravity of valence and conduction bands), the "dielectric midgap energy,"[33] the deep-impurity levels,[32] etc. to which we may add on an empirical basis the pinned Fermi level (approximate equal to center of gravity of surface states). The band lineups deduced from their alignment are in ≈0.1 eV agreement with each other. Indeed, it has been pointed out[40] that such levels are naturally pinned to each other, and also related to the intrinsic Fermi level, the minimum of density of states, the Fermi level in the amorphous material, the center of gravity of bonding and antibonding states of dangling bonds, etc. It may be then put forward that on an absolute energy scale the band structures of all III-V compounds align their main features: vacuum level, near-atomic core levels (cf. ternary alloys and structures), center of gravity of bulk and surface states (cf. stability of Fermi level), etc. During the formation of heterointerfaces, no charge transfer and then no shift of the substrate band structure occurs, and this alignment fixes the band offset. Similarly, as pointed out by Tersoff,[31] during the formation of metal-semiconductor contacts, the Fermi level of the metal aligns with the neutral level of the semiconductor for the same interface neutrality condition, thus fixing the Schottky barrier. Our presentation is obviously oversimplified and needs a deeper theoretical basis, but it encompasses all experimental data with a fair accuracy.

Simple energy determinations by (*in situ*) surface techniques may then lead to good first-basis predictions of band lineup in other systems (III-V ternary and quaternary compounds, II-VI, etc.) with the ultimate goal of band-gap engineering. Indeed, data on Ge/Si (Ref. 41) suggest that a similar approach may also apply to fourth-column elemental semiconductors. Finally, from a different point of view, the predictability of surface states can be used for engineering the surface electronic properties as we suggested earlier,[42] by fitting on the desired bulk the "surface" formed by a ML-thick overlayer with the material having the desired surface properties.

VI. CONCLUSION

By molecular-beam-epitaxy techniques, we have built ultrathin III-V overlayers on III-V substrates, which are the first steps of heterojunction buildup. For selected couples excluding those where surface segregation occurs and blurs the interface, the morphology of these structures is planar and their composition gradient abrupt at the submonolayer level. The surface reconstruction is controlled mainly by the nature of the surface layer and by the lattice mismatch between overlayer and substrate materials, and is altered when this mismatch lies above $\approx 3\%$. On the other hand, occupied and empty states associated with the overlayer do not depend on this mismatch and are located at the energies where the valence and conduction bands and surface states of thick overlayers lie; they may then be considered as precursors of these bands, rather unaltered by the underlying substrate. This stability may be potentially used for surface engineering purposes, since desired surface properties can be obtained by fitting on the bulk material a ML-thick layer of the material having these desired properties. With respect to the vacuum level, we also find that the substrate band structure is also stationary during the heterojunction buildup, which confirms the "revival" of the electron-affinity rule for band-offset determination. This behavior may be possibly restricted to the chemically and structurally similar III-V compounds, though similar indications exist for IV-column materials. Finally, our results contribute to suggest a common origin for the Fermi-level pinning at free surfaces, the band lineup in heterojunctions, and the barrier height at metal-semiconductor contacts.

ACKNOWLEDGMENTS

We gratefully acknowledge fruitful discussions with C. A. Sébenne, J. Y. Marzin, D. Paquet, and R. Resta. One of us (C. Guille) has benefited from a grant of the French Ministry of Research and Technology. Laboratoire de Bagneux is Unité No. 250 associée au Centre National de la Recherche Scientifique (France).

[1] *Heterojunction Band Discontinuities,* edited by F. Capasso and G. Margaritondo (North-Holland, Amsterdam, 1987).

[2] J. R. Waldrop, S. P. Kowalczyk, R. W. Grant, E. A. Kraut, and D. L. Miller, J. Vac. Sci. Technol. **19**, 573 (1981); S. P. Kowalczyk, W. J. Schaffer, E. A. Kraut, and R. W. Grant, *ibid.* **20**, 705 (1982); A. D. Katnami and R. S. Bauer, Phys. Rev. B **33**, 1106 (1986); J. R. Waldrop, R. W. Grant, and E. A. Kraut, J. Vac. Sci. Technol. B **5**, 1209 (1987); D. W. Niles, B. Lai, J. T. McKinley, G. Margaritondo, G. Wells, F. Cerrina, G. J. Gualtieri, and G. P. Schwartz, *ibid.* B **5**, 1286 (1987).

[3] J. M. Moison, M. Bensoussan, and F. Houzay, Phys. Rev. B **34**, 2018 (1986), and references therein.

[4] See, for instance, *The Technology and Physics of Molecular Beam Epitaxy,* edited by E. H. C. Parker (Plenum, New York, 1985).

[5] J. M. Moison, M. Van Rompay, and M. Bensoussan, Appl. Phys. Lett. **48**, 1362 (1986).

[6] See, for instance, R. People and J. C. Bean, Appl. Phys. Lett. **47**, 322 (1985).

[7] B. W. Dodson, Phys. Rev. B **30**, 3545 (1984); T. Hibma, in *The Structure of Surfaces,* Vol. 11 of *Springer Series in Surface Science,* edited by J. F. Van der Veen and M. A. Van Hove (Springer-Verlag, Berlin, 1988), p. 419.

[8] T. Narusawa and W. M. Gibson, J. Vac. Sci. Technol. **20**, 709 (1982); J. C. Bean, L. C. Feldman, A. T. Fiory, S. Nakahara, and I. K. Robinson, *ibid.* A **2**, 436 (1984); H. J. Gossmann, L. C. Feldman, and W. M. Gibson, Surf. Sci. **155**, 413 (1985).

[9] F. Houzay, C. Guille, J. M. Moison, P. Hénoc, and F. Barthe, J. Cryst. Growth **81**, 67 (1987).

[10] A review of data on surface segregation in heterostructures is presented by one of us (J. M. Moison), in *Advanced Materials for Telecommunications,* edited by P. A. Glassow, Y. I. Nissim, J. P. Noblanc, and J. Speight (Les Editions de Physique, Les Ulis, 1986); more recent data may be found in J. Massiès, F. Turco, A. Salettes, and J. P. Contour, J. Cryst. Growth **80**, 307 (1987). The neighboring problem of surface segregation at metal-semiconductor interfaces has recently been reviewed by Z. Lin, F. Xu, and J. H. Weaver, Phys. Rev. B **36**, 5777 (1987).

[11] C. Guille, F. Houzay, J. M. Moison, and F. Barthe, Surf. Sci. **189/190**, 1041 (1987).

[12] B. Deveaux, J. Y. Emery, A. Chomette, B. Lambert, and M. Baudet, Appl. Phys. Lett. **45**, 1078 (1984).

[13] S. M. Newstead, R. A. A. Kubiak, and E. H. C. Parker, J. Cryst. Growth **81**, 49 (1987).

[14] J. M. Moison, C. Guille, and M. Bensoussan, Phys. Rev. Lett. **58**, 2555 (1987).

[15] J. C. Phillips, Phys. Rev. Lett. **45**, 905 (1980); D. Vanderbilt, Phys. Rev. B **36**, 6209 (1987).

[16] W. Gudat and D. E. Eastman, in *Photoemission and the Electronic Properties of Surfaces,* edited by B. Feuerbacher, B. Fitton, and R. F. Willis (Wiley, New York, 1978), pp. 315–352.

[17] J. R. Chelikowsky and M. Cohen, Phys. Rev. B **14**, 555 (1976).

[18] P. K. Larsen, J. H. Neave, J. F. Van der Veen, P. J. Dobson, and B. A. Joyce, Phys. Rev. B **27**, 4966 (1983); G. M. Guichar, C. A. Sébenne, and C. D. Thuault, J. Vac. Sci. Technol. **16**, 1212 (1979); J. M. Moison and M. Bensoussan, Surf. Sci. **168**, 68 (1986).

[19] *Photoemission in Solids,* edited by M. Cardona and L. Ley (Springer-Verlag, Berlin, 1978), p. 25.

[20] C. D. Thuault, G. M. Guichar, and C. A. Sébenne, Surf. Sci. **80**, 273 (1979); G. M. Guichar, C. A. Sébenne, and C. D.

Thuault, *ibid.* **86**, 789 (1979).
[21]A. D. Katnami and G. Margaritondo, Phys. Rev. B **28**, 1944 (1983).
[22]P. K. Larsen, J. H. Neave, J. F. van der Veen, P. J. Dobson, and B. A. Joyce, Phys. Rev. B **27**, 4966 (1983); R. Z. Bachrach, R. S. Bauer, P. Chiaradia, and G. V. Hansson, J. Vac. Sci. Technol. **19**, 335 (1981).
[23]C. K. Shih and W. E. Spicer, Phys. Rev. Lett. **58**, 2594 (1987); J. Hwang, P. Pianetta, C. K. Shih, W. E. Spicer, Y. C. Pao, and J. S. Harris, Appl. Phys. Lett. **51**, 1632 (1987).
[24]R. Ludeke and L. Esaki, Surf. Sci. **47**, 132 (1975); J. Van Laar, A. Huijser, and T. L. Van Rooy, J. Vac. Sci. Technol. **14**, 894 (1977); R. Ludeke, IBM J. Res. Dev. **22**, 304 (1978).
[25]W. Gudat and D. E. Eastman, J. Vac. Sci. Technol. **13**, 831 (1976).
[26]G. L. Bir and G. E. Pikus, *Symmetry and Strain-Induced Effects in Semiconductors* (Wiley, New York, 1974).
[27]C. G. Van de Walle and R. M. Martin, J. Vac. Sci. Technol. B **3**, 1256 (1985).
[28]H. Kroemer, J. Vac. Sci. Technol. B **2**, 433 (1984).
[29]G. Margaritondo, Surf. Sci. **168**, 439 (1986).
[30]J. C. Duran, F. Flores, C. Tejedor, and A. Munoz, Phys. Rev. B **36**, 5920 (1987); B. Haussy, C. Priester, G. Allan, and M. Lannoo, *ibid.* **36**, 1105 (1987); C. Van de Walle and R. M. Martin, *ibid.* **35**, 8154 (1987); A. Baldereschi, S. Baroni, and R. Resta, Phys. Rev. Lett. **61**, 734 (1988).
[31]J. Tersoff, Phys. Rev. Lett. **56**, 2755 (1986).
[32]J. M. Langer and H. Heinrich, Phys. Rev. Lett. **55**, 1414 (1985), Physica B+C **134B**, 444 (1985); in *Proceedings of the 18th Conference on the Physics of Semiconductors, Stockholm, 1986,* edited by O. Engström (World Scientific, Singapore, 1987), p. 175.
[33]M. Cardona and N. E. Christensen, Phys. Rev. B **35**, 6182 (1987).
[34]G. Margaritondo and P. Perfetti, in Ref. 1, p. 72.
[35]B. Haussy, C. Priester, G. Allan, and M. Lannoo, in Ref. 32, p. 171.
[36]W. A. Harrison and J. Tersoff, J. Vac. Sci. Technol. B **4**, 1068 (1986).
[37]C. A. Sébenne, D. Bolmont, G. Guichar, and M. Balkanski, Phys. Rev. B **12**, 3280 (1975); G. M. Guichar, G. A. Garry, and C. Sébenne, Surf. Sci. **85**, 326 (1979).
[38]E. A. Kraut, J. Vac. Sci. Technol. B **5**, 1246 (1987).
[39]C. Mailhiot and C. B. Duke, J. Vac. Sci. Technol. A **4**, 869 (1986).
[40]J. Tersoff and W. A. Harrison, J. Vac. Sci. Technol. B **5**, 1221 (1987).
[41]P. Cheng, D. Bolmont, and C. A. Sébenne, Solid State Commun. **46**, 689 (1983).
[42]J. M. Moison, M. Van Rompay, C. Guille, F. Houzay, F. Barthe, and M. Bensoussan, in Ref. 32, p. 105; J. M. Moison, in *Semiconductor Interfaces: Formation and Properties,* Vol. 22 of *Springer Proceedings in Physics,* edited by G. Le Lay (Springer, Berlin, 1987).

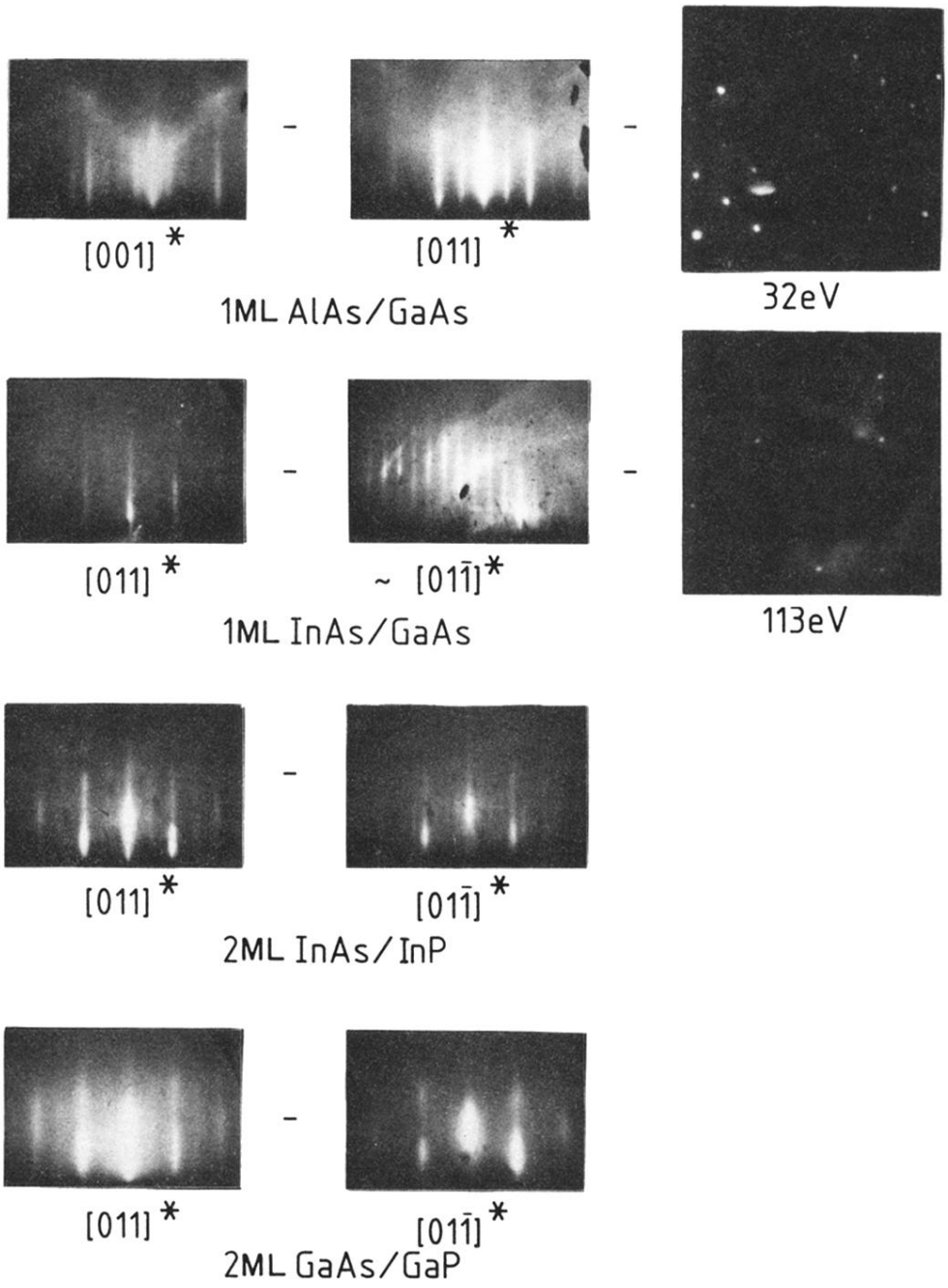

FIG. 1. Room-temperature electron-diffraction patterns of various overlayer-substrate structures: $c(4\times4)1$ ML AlAs/GaAs, $(2\times3)1$ ML InAs/GaAs, $(2\times4)2$ ML InAs/InP, and $(2\times4)2$ ML GaAs/GaP. The primary energy is 10 keV for RHEED patterns and is indicated under each picture for LEED patterns. Crystallographic directions indicated for RHEED patterns are normal to the picture plane.